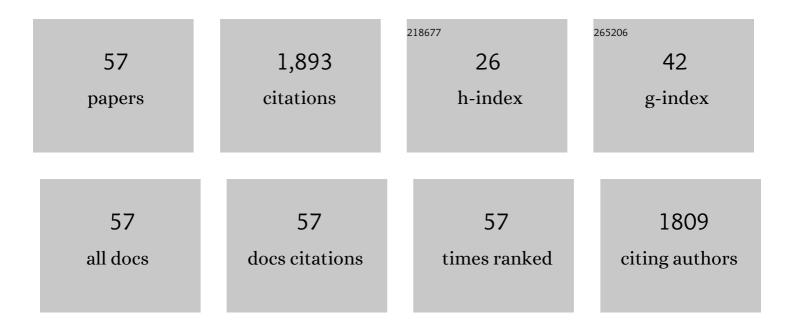
List of Publications by Year in descending order

Source: https://exaly.com/author-pdf/709615/publications.pdf Version: 2024-02-01



WENZHIL

#	Article	IF	CITATIONS
1	Catalytic conversion of xylose and corn stalk into furfural over carbon solid acid catalyst in Î <sup>3</sup> -valerolactone. Bioresource Technology, 2016, 209, 108-114.	9.6	127
2	Typical crystal face effects of different morphology ceria on the activity of Pd/CeO2 catalysts for lean methane combustion. Fuel, 2018, 233, 10-20.	6.4	103
3	Conversion of corn stalk into furfural using a novel heterogeneous strong acid catalyst in γ-valerolactone. Bioresource Technology, 2015, 198, 764-771.	9.6	90
4	Enhanced furfural production from raw corn stover employing a novel heterogeneous acid catalyst. Bioresource Technology, 2017, 245, 258-265.	9.6	88
5	Selective oxidation of 5-hydroxymethylfurfural to 2,5-furandicarboxylic acid over Au/CeO <sub>2</sub> catalysts: the morphology effect of CeO <sub>2</sub> . Catalysis Science and Technology, 2019, 9, 1570-1580.	4.1	77
6	Pretreatment of corn stover for sugar production using a two-stage dilute acid followed by wet-milling pretreatment process. Bioresource Technology, 2016, 211, 435-442.	9.6	76
7	Efficient transformation of corn stover to furfural using p-hydroxybenzenesulfonic acid-formaldehyde resin solid acid. Bioresource Technology, 2018, 264, 261-267.	9.6	70
8	Liquefaction of kraft lignin by hydrocracking with simultaneous use of a novel dual acid-base catalyst and a hydrogenation catalyst. Bioresource Technology, 2017, 243, 100-106.	9.6	69
9	Recent advances in catalytic production of sugar alcohols and their applications. Science China Chemistry, 2017, 60, 853-869.	8.2	68
10	Production of liquid fuel intermediates from furfural via aldol condensation over Lewis acid zeolite catalysts. Catalysis Science and Technology, 2017, 7, 3555-3561.	4.1	66
11	High conversion of glucose to 5-hydroxymethylfurfural using hydrochloric acid as a catalyst and sodium chloride as a promoter in a water/Î <sup>3</sup> -valerolactone system. RSC Advances, 2017, 7, 14330-14336.	3.6	64
12	Dehydration of glucose to 5-hydroxymethylfurfural and 5-ethoxymethylfurfural by combining Lewis and BrĄ̈,nsted acid. RSC Advances, 2017, 7, 41546-41551.	3.6	59
13	Production of furfural from xylose and corn stover catalyzed by a novel porous carbon solid acid in Î <sup>3</sup> -valerolactone. RSC Advances, 2017, 7, 29916-29924.	3.6	57
14	A two-stage pretreatment process using dilute hydrochloric acid followed by Fenton oxidation to improve sugar recovery from corn stover. Bioresource Technology, 2016, 219, 753-756.	9.6	55
15	Production of liquefied fuel from depolymerization of kraft lignin over a novel modified nickel/H-beta catalyst. Bioresource Technology, 2018, 269, 346-354.	9.6	51
16	Oneâ€Pot Conversion of Carbohydrates into 5â€(Hydroxymethyl)furfural using Heterogeneous Lewisâ€Acid and BrÃ,nstedâ€Acid Catalysts. Energy Technology, 2017, 5, 747-755.	3.8	41
17	Atomically dispersed palladium-based catalysts obtained <i>via</i> constructing a spatial structure with high performance for lean methane combustion. Journal of Materials Chemistry A, 2020, 8, 7395-7404.	10.3	40
18	Hydroxyl groups attached to Co <sup>2+</sup> on the surface of Co <sub>3</sub> O <sub>4</sub> : a promising structure for propane catalytic oxidation. Catalysis Science and Technology, 2020, 10, 2573-2582.	4.1	39

#	Article	IF	CITATIONS
19	HCHO Removal by MnO <sub>2</sub> ( <i>x</i> )–CeO <sub>2</sub> : Influence of the Synergistic Effect on the Catalytic Activity. Industrial & Engineering Chemistry Research, 2020, 59, 596-608.	3.7	38
20	Efficient depolymerization of Kraft lignin to liquid fuels over an amorphous titanium-zirconium mixed oxide supported partially reduced nickel-cobalt catalyst. Bioresource Technology, 2019, 284, 293-301.	9.6	36
21	Lignin-first depolymerization of native corn stover with an unsupported MoS <sub>2</sub> catalyst. RSC Advances, 2018, 8, 1361-1370.	3.6	35
22	Recent progress in direct production of furfural from lignocellulosic residues and hemicellulose. Bioresource Technology, 2022, 354, 127126.	9.6	34
23	Efficient catalytic conversion of corn stover to furfural and 5-hydromethylfurfural using glucosamine hydrochloride derived carbon solid acid in $\mathcal{E}^3$ -valerolactone. Industrial Crops and Products, 2021, 161, 113173.	5.2	33
24	Production of high-yield short-chain oligomers from cellulose <i>via</i> selective hydrolysis in molten salt hydrates and separation. Green Chemistry, 2019, 21, 5030-5038.	9.0	32
25	p-Hydroxybenzenesulfonic acid–formaldehyde solid acid resin for the conversion of fructose and glucose to 5-hydroxymethylfurfural. RSC Advances, 2017, 7, 27682-27688.	3.6	31
26	Synthesis of sulfonated chitosan-derived carbon-based catalysts and their applications in the production of 5-hydroxymethylfurfural. International Journal of Biological Macromolecules, 2020, 157, 368-376.	7.5	30
27	A two-stage pretreatment using acidic dioxane followed by dilute hydrochloric acid on sugar production from corn stover. RSC Advances, 2017, 7, 32452-32460.	3.6	27
28	Palladium Nanoparticles Supported on Surface-Modified Metal Oxides for Catalytic Oxidation of Lean Methane. ACS Applied Nano Materials, 2020, 3, 12130-12138.	5.0	27
29	Low Temperature Complete Combustion of Lean Methane over Cobalt–Nickel Mixedâ€Oxide Catalysts. Energy Technology, 2017, 5, 604-610.	3.8	26
30	Efficient catalytic conversion of corn stalk and xylose into furfural over sulfonated graphene in Î <sup>3</sup> -valerolactone. RSC Advances, 2019, 9, 10569-10577.	3.6	26
31	Ultrafast Glycerol Conversion to Lactic Acid over Magnetically Recoverable Ni–NiO <i><sub>x</sub></i> @C Catalysts. Industrial & Engineering Chemistry Research, 2020, 59, 9912-9925.	3.7	26
32	Highly active Pd catalysts supported on surface-modified cobalt-nickel mixed oxides for low temperature oxidation of lean methane. Fuel, 2020, 279, 118372.	6.4	26
33	Conversion of biomass-derived carbohydrates into 5-hydroxymethylfurfural catalyzed by sulfonic acid-functionalized carbon material with high strong-acid density in Î <sup>3</sup> -valerolactone. Research on Chemical Intermediates, 2018, 44, 5439-5453.	2.7	18
34	Production of furfural from xylose catalyzed by a novel calcium gluconate derived carbon solid acid in 1,4-dioxane. New Journal of Chemistry, 2020, 44, 7968-7975.	2.8	18
35	Characterization Of C <sub>60</sub> /Bi <sub>2</sub> TiO <sub>4</sub> F <sub>2</sub> as a Potential Visible Spectrum Photocatalyst for The Depolymerization of Lignin. Journal of Wood Chemistry and Technology, 2016, 36, 365-376.	1.7	15
36	Efficient Synthesis of Liquid Fuel Intermediates from Furfural and Levulinic Acid via Aldol Condensation over Hierarchical MFI Zeolite Catalyst. Energy & Fuels, 2019, 33, 12518-12526.	5.1	15

#	Article	IF	CITATIONS
37	Catalytic Performance of Novel Hierarchical Porous Flower-Like NiCo2O4 Supported Pd in Lean Methane Oxidation. Catalysis Letters, 2018, 148, 2799-2811.	2.6	13
38	High performance of Mo-promoted Ir/SiO2 catalysts combined with HZSM-5 toward the conversion of cellulose to C5/C6 alkanes. Bioresource Technology, 2020, 297, 122492.	9.6	13
39	Highly Active and Stable Palladium Catalysts Supported on Surfaceâ€modified Ceria Nanowires for Lean Methane Combustion. ChemCatChem, 2021, 13, 664-673.	3.7	13
40	Pentaâ€coordinated Al <sup>3+</sup> Stabilized Defectâ€Rich Ceria on Al <sub>2</sub> O <sub>3</sub> Supported Palladium Catalysts for Lean Methane Oxidation. ChemCatChem, 2021, 13, 3490-3500.	3.7	13
41	Impact of ferrocene on the nanostructure and functional groups of soot in a propane/oxygen diffusion flame. RSC Advances, 2017, 7, 5427-5436.	3.6	11
42	Preparation of two different crystal structures of cerous phosphate as solid acid catalysts: their different catalytic performance in the aldol condensation reaction between furfural and acetone. RSC Advances, 2019, 9, 16919-16928.	3.6	11
43	Continuous Production of 5â€Hydroxymethylfurfural from Monosaccharide over Zirconium Phosphates. ChemistrySelect, 2018, 3, 10983-10990.	1.5	9
44	Au Nanoparticles Supported on Iron-Based Oxides for Soot Oxidation: Physicochemical Properties Before and After the Reaction. ACS Omega, 2021, 6, 11510-11518.	3.5	8
45	Elucidation of the Active Phase in Pdâ€Based Catalysts Supporting on Octahedral CeO <sub>2</sub> for Lowâ€Temperature Methane Oxidation. ChemistrySelect, 2021, 6, 4149-4159.	1.5	8
46	Efficient conversion of corn stover to 5-hydroxymethylfurfural and furfural using a novel acidic resin catalyst in water-1, 4-dioxane system. Molecular Catalysis, 2021, 515, 111920.	2.0	8
47	Degradation of Formaldehyde over MnO <sub>2</sub> /CeO <sub>2</sub> Hollow Spheres: Elucidating the Influence of Carbon Sphere Self-Sacrificing Templates. ACS Omega, 2021, 6, 35404-35415.	3.5	8
48	High dispersed Pd supported on CeO2 (1 0 0) for CO oxidation at low temperature. Molecular Catalysis, 2021, 508, 111580.	2.0	7
49	Liquid membrane catalytic model of hydrolyzing cellulose into 5-hydroxymethylfurfural based on the lattice Boltzmann method. RSC Advances, 2019, 9, 12846-12853.	3.6	6
50	Catalytic Conversion of Glucose to 5-Hydroxymethylfurfural and Furfural by a Phosphate-Doped SnO2 Catalyst in γ-Valerolactone-Water System. Catalysis Letters, 2020, 150, 3304-3313.	2.6	6
51	A rod-like Co3O4 with high efficiency and large specific surface area for lean methane catalytic oxidation. Molecular Catalysis, 2022, 522, 112229.	2.0	6
52	Valorization of lignin in native corn stover via fractionation-hydrogenolysis process over cobalt-supported catalyst without external hydrogen. Molecular Catalysis, 2021, 514, 111832.	2.0	5
53	Coking Prediction in Catalytic Glucose Conversion to Levulinic Acid Using Improved Lattice Boltzmann Model. Industrial & Engineering Chemistry Research, 2020, 59, 17462-17475.	3.7	4
54	Effects of the novel catalyst Ni–S <sub>2</sub> O <sub>8</sub> <sup>2â~`</sup> –K <sub>2</sub> O/TiO <sub>2</sub> on efficient lignin depolymerization. RSC Advances, 2020, 10, 8558-8567.	3.6	4

#	Article	IF	CITATIONS
55	Tungsten oxide decorated silica-supported iridium catalysts combined with HZSM-5 toward the selective conversion of cellulose to C6 alkanes. Bioresource Technology, 2022, 347, 126403.	9.6	3
56	The effects of facet-dependent palladium-titania interactions on the activity of Pd/Rutile catalysts for lean methane oxidation. Molecular Catalysis, 2022, 528, 112475.	2.0	3
57	Numerical Studies on Cellulose Hydrolysis in Organic–Liquid–Solid Phase Systems with a Liquid Membrane Catalysis Model. ACS Omega, 2022, 7, 2286-2303.	3.5	1